Research Article

Centimeter scale color printing with grayscale lithography

Yu Chen,[a,†] **Yang Li,**[a,†] **Wenhao Tang,**[a,†] **Yutao Tang,**[a] **Yue Hu,**[a] **Zixian Hu,**[a] **Junhong Deng,**[b] **Kokwai Cheah**[c] **and Guixin Li**[a,*]

[a]Southern University of Science and Technology, Department of Materials Science and Engineering, Shenzhen, China
[b]Southern University of Science and Technology, Shenzhen Institute for Quantum Science and Engineering, Shenzhen, China
[c]Hong Kong Baptist University, Department of Physics and Institute of Advanced Materials, Hong Kong, China

Abstract. Structural color from artificial structures, due to its environmental friendliness and excellent durability, represents a route for color printing applications. Among various physical mechanisms, the Fabry–Perot (F–P) cavity effect provides a powerful way to generate vivid colors in either the reflection or transmission direction. Most of the previous F–P type color printing works rely on electron beam grayscale lithography, however, with this technique it is challenging to make large-area and low-cost devices. To circumvent this constraint, we propose to fabricate the F–P type color printing device by the laser grayscale lithography process. The F–P cavity consists of two thin silver films as mirrors and a photoresist film with a spatially variant thickness as the spacer layer. By controlling the laser exposure dose pixel by pixel, a centimeter-scale full-color printing device with a spatial resolution up to $5~\mu\text{m} \times 5~\mu\text{m}$ is demonstrated. The proposed large area color printing device may have great potential in practical application areas such as color displays, hyperspectral imaging, advanced painting, and so on.

Keywords: structural color; laser grayscale lithography; Fabry–Perot cavity.

1 Introduction

Compared with the conventional painting technology with chemical dyes, structural color from artificial mediums has broader application ranges and thus becomes a more attractive color management technology.[1] It is also environmentally friendly and durable. For some applications, the color management requires a high spectral resolution or a controllable spectral bandwidth. In these scenarios, the design of artificial photonic devices relies on various physical mechanisms such as multilayer interference,[2,3] diffraction,[4] plasmonic resonance,[5–11] and Fabry–Perot (F–P) cavity effects.[12,13] One of the representative color management devices is photonic crystals, which consist of periodic unit cells.[14] However, the periodic photonic crystal structures are difficult to be used for color printing, which usually requires spatially variant distribution of the artificial structures. Alternatively, the dielectric metasurfaces,[15–22] which can be fabricated by using electron beam lithography (EBL), can be used for color printing. However, the fabrication of these kinds of color printing devices is usually time-consuming and has a small size, which may limit the practical applications.

Among various design concepts of the color printing technology, the F–P cavity effect has been attracting scientific attention. Compared with most of the plasmonic and dielectric metasurface devices, colors generated from the F–P cavity usually have less crosstalk. For color printing applications, the reflection[23–28] or transmission-type[29–31] F–P cavities with spatially variant spacer thickness have been widely investigated. In previous works, the fabrication of pixelated F–P cavities mainly relies on electron beam lithography (EBL) and related processes. The EBL-based technique has a high spatial resolution; however, the fabrication process is usually time-consuming and thus most of the reported sample sizes are limited to submillimeter scale. By using the binary mask and lateral translation process, one can achieve fast pattern transfer for mass production applications. However, this

*Address all correspondence to Guixin Li, ligx@sustech.edu.cn
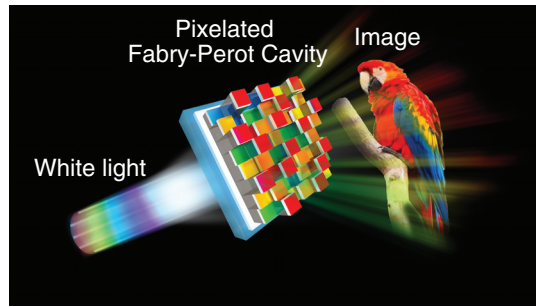
†These authors contributed equally.

Fig. 1 Schematic diagram of the working principle of the color printing by using pixelated F–P cavities. The F–P cavity consists of a silver (Ag)/PR/silver (Ag) sandwich structure. The spatially variant thickness of the PR layer is realized through the laser grayscale lithography process. Under the illumination of a white light source, the colorful image with a micron-scale spatial resolution can be obtained.

kind of fabrication procedure is complicated and requires critical alignment between two exposure steps.[31] In comparison, the shadow mask method can be used to make large area color printing devices with low spatial resolution and limited color components.[27] Therefore, fast manufacturing of the large area F–P type color printing device with a high spatial resolution remains challenging.

Here, we develop a fast color printing technique by using the concept of pixelated F–P cavities and the laser grayscale lithography process. In this technique, the colorful image with multiple color components is first converted to a predefined grayscale pattern and then engraved on the photoresist (PR) layer by controlling the exposure dose during the grayscale laser writing process. As shown in Fig. 1, the pixelated PR spacer layers are sandwiched by two semitransparent sliver thin films to form the transmission type F–P cavities. Under the illumination of a white light source, the transmission color can be continuously tuned in the visible spectral regime by finely controlling the thickness of the PR layer. We show that a centimeter-scale color printing device with a pixel size of 5 $\mu m \times 5$ μm can be fabricated at a record speed of $\sim 10^4$ $\mu m^2/s$, with a total time of ~ 170 min. In the visible regime, the transmission efficiency of the fabricated F–P cavities is between 39% and 50%, which is comparable to that of the EBL-based devices. It should be noted that the pixelated F–P cavity in transmission mode is also an excellent candidate for making color filter arrays, which can be used for spectral imaging. Last, but not least, the large area color filter arrays with various pixel sizes are also demonstrated. It can be found that the newly developed laser grayscale lithography process in this work well leverages the fabrication speed and the spatial resolution of pixelated F–P cavities. All these efforts make it feasible to produce large area and high-resolution color printing devices and color filters for applications in imaging and wearable devices.

2 Results and Discussion

2.1 Calculated Optical Properties of the Fabry–Perot Cavities

Figure 2(a) shows the schematic diagram of the F–P cavity, which consists of a silver (Ag)/ PR/silver (Ag) sandwich structure. The F–P cavity is sitting on a glass substrate. To balance

the transmission efficiency and the bandwidth of the transmission peak, the thickness of each silver layer is chosen to be 30 nm. To avoid the oxidation of silver, a SiO_2 encapsulation layer is coated on top of the F–P cavity. To simplify the design and fabrication process, the thickness of the SiO_2 layer, which can affect the transmission property of the cavity, is fixed at 20 nm. Under normal incidence, we numerically calculated the transmission spectra of the F–P cavities with different PR thicknesses. Figure 2(b) shows the typical transmission spectra of the R, G, and B F–P cavities with spacer thicknesses of 138, 105, and 79 nm, respectively. It can be found that the bandwidth of the color filter at longer wavelengths becomes narrower, which is mainly because of the dispersion of silver in the visible spectral region. By scanning the PR thickness L from 60 to 160 nm, the resonant wavelengths can be continuously tuned in the visible spectral regime [Fig. 2(c)]. In Fig. 2(d), the colors (black circles), which are calculated from the simulation results in Fig. 2(c), are mapped to the International Commission on Illumination (CIE) 1931 xy chromaticity diagram. It is shown that the Ag/PR/Ag-based F–P cavities can provide a broadband color range for color printing applications. It should be noted that the transmission peaks will change under oblique incidence;[12] however, this is not the focus of the current work.

2.2 Fabrication and Characterization of the Color Palettes

To experimentally verify the optical properties of the F–P cavities, we fabricate a series of color palettes by using the laser grayscale lithography process (Fig. S5, Supplemental Material). The grayscale photolithography process is based on the commercial direct laser writing equipment from Heidelberg Instruments. The fabrication process includes the following steps: first, a silver layer with a thickness of ~ 30 nm was deposited on a glass substrate, then the PR layer with a thickness of ~ 150 nm was spin-coated on top of the silver. The thickness of the spatially variant PR spacer layer can be controlled by varying the exposure dose of a 405 nm laser. After that, the second silver layer with a thickness of 30 nm and a SiO_2 encapsulation layer with a thickness of 20 nm was deposited onto the patterned PR layer by using the electron beam evaporation method.

Then, we characterize the optical performance of the color palettes. As shown in Fig. 3(a), under the illumination of a white light source, the photos of the color palettes with different PR thicknesses L are taken by using a Canon camera (Fig. S3, Supplemental Material). The white-balanced photos show that the blue, green, yellow, and red colors can be easily obtained by varying L from 83 to 149 nm. In addition, the transmission efficiency of the F–P cavities is summarized in Fig. 3(b). For the F–P cavities working in the visible regime, the transmission efficiencies are between 39% and 50%. It is found that the measured transmission efficiencies are lower than that of calculated ones in Fig. 2. This may be because the imaginary part of the refractive index of the PR used in the numerical model is smaller than that in the real device. The full width at half maximum (FWHM) of the transmission peaks for the red, green, and blue F–P cavities are ~ 37, 51, and 87 nm, respectively. The bandwidths of the three color filters are narrower than that of commercial products from Thorlabs.[32] The calculated transmission efficiency at blue wavelengths is higher than that at longer wavelengths. However, the measured transmission spectra have
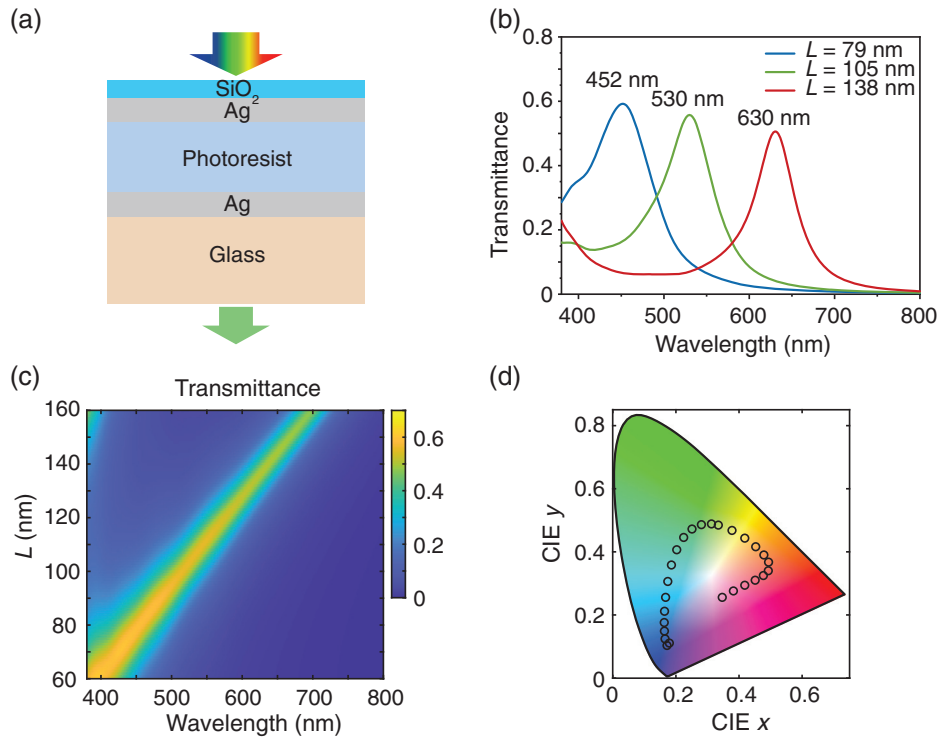
Fig. 2 Calculated optical responses of the silver (Ag)/PR/silver (Ag) F–P cavities. (a) The cross-section of the F–P cavity. The silver film with a thickness of 30 nm and the PR layer serve as the mirror and the spacer of the F–P cavity, respectively. The F–P cavity sitting on the glass substrate is encapsulated by a 20-nm-thick SiO_2 layer to avoid the oxidation of the silver layer. (b) Transmission spectra of the F–P cavities working at red (630 nm), green (530 nm), and blue (452 nm) wavelengths; the corresponding cavity lengths are 138, 105, and 79 nm, respectively. (c) The transmission efficiency as a function of spacer thickness and wavelength is plotted. (d) The calculated transmission colors labeled with black circles are mapped in the CIE 1931 chromaticity diagram.
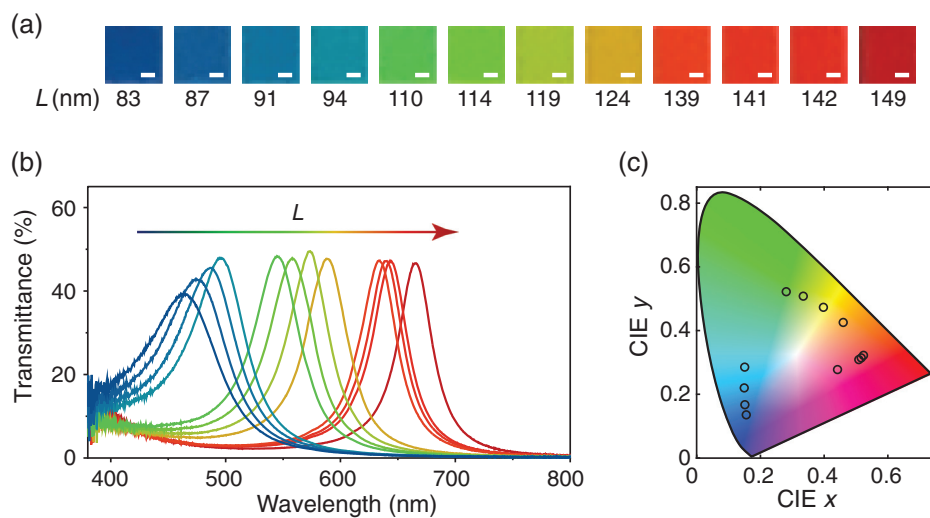

Fig. 3 Optical properties of the color palettes. (a) Under the illumination of a halogen lamp, the white-balanced photos of the color palettes are taken by using a commercial camera. L is the retrieved effective length of the PR layer. The scale bar is 50 μm. (b) Measured transmission spectra of the color palettes in which the PR layers have different thicknesses. The colors of lines are corresponded to (a). (c) The measured transmission colors (black circles) are mapped in the CIE 1931 chromaticity diagram.
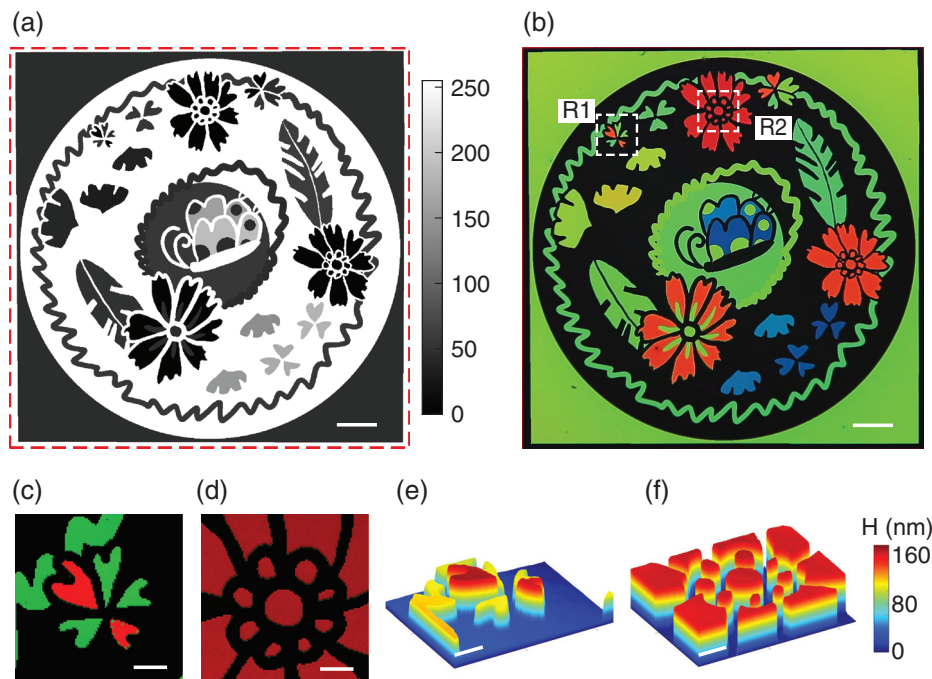
Fig. 4 Centimeter scale color printing with the pixelated F–P cavities. (a) The grayscale figure is converted from the original drawing. (b) Under the illumination of a halogen lamp, the white balanced photo of the centimeter scale color printing device. (c) and (d) The microscopy images of the regions R1 and R2, which are shown by the white dashed box in (b). (e) and (f) The 3D profiles of the regions R1 and R2, which are measured by using a white light interferometer. The scale bars in (a) and (b) are 1 mm. The scale bars in (c), (d), (e), and (f) are 200 μm.

a reversed trend. This phenomenon should come from the change in the refractive index of the PR layer before and after laser exposure. As demonstrated in Fig. 3(c), the transmission colors of the palettes form a wide gamut in the CIE 1931 chromaticity diagram, which means that the proposed F–P cavities can be used for color printing applications.

2.3 Centimeter Scale Color Printing

To verify the color printing application of the laser grayscale lithography process, we demonstrate the ability to make a centimeter-scale full-color device. Based on the optical properties of the color palettes in the previous section, we roughly know the relationship between the grayscale values that were used to expose the PR layer and the transmission color. As shown in Fig. 4(a), a colorful drawing can be represented by a pixelated figure with spatially variant grayscale values from 0 to 255. This grayscale figure was then imported into the laser direct writing equipment to control the PR thickness in a one-step photolithography process. The grayscale patterning speed is up to 10^4 μm^2 s^{-1}. The 30-nm thick top silver mirror and the 20-nm thick SiO$_2$ capping layer were subsequently deposited.

Figure 4(b) shows the white balanced digital photo of the centimeter scale color printing device which is illuminated by a halogen lamp. The pixel size of the device is 5 μm × 5 μm, and the size of the printing is around 10 mm × 10 mm. Various transmission colors are achieved without any color mixture. Figures 4(c) and 4(d) show the microscopy images of regions R1 and R2 in Fig. 4(b), and the sharp edges indicate that the high-resolution color printing can be achieved. In addition,

we also conducted the white light interferometry measurement. From the three-dimensional profile in Figs. 4(e) and 4(f), we can easily extract the height of the pixelated F–P cavities.

2.4 Color Filter Arrays

Another important application of the F–P cavities is color filter arrays, which are the critical components in the areas of colorful imaging, liquid crystal display, and so on. The conventional color filter arrays for imaging sensors and flat panel display are usually manufactured by using dye-doped color resist.[33–35] However, the chemical dyes usually have poor durability, and the fabrication of the color filters involves multiple photolithography processes. In comparison, the spatially variant large area F–P cavities can be used to design the color filter arrays. To verify this idea, we designed a color filter array with a size of 3.6 mm × 4.8 mm, which is equivalent to the size of a 1/3-in. Complementary metal-oxide-semiconductor (CMOS) sensor (Fig. S8, Supplemental Material). The color filter array is composed of periodic unit cells, and each unit cell includes four pixels: red (669 nm), yellow (591 nm), green (545 nm), and blue (468 nm), which are arranged in a 2 × 2 lattice. The transmission efficiency for the four kinds of color filters is 46.6%, 48.3%, 47.4%, and 38.4%, respectively. The size of the pixels varies from 30 μm × 30 μm to 5 μm × 5 μm. Figure 5 shows the microscopy images of the color filter arrays. It is found that the pixel shape and color uniformity deviates from an ideal one when the pixel size becomes smaller, which should be due to the proximity effect in the laser writing process and the systematic error of the equipment. For the F–P cavity with pixel size of
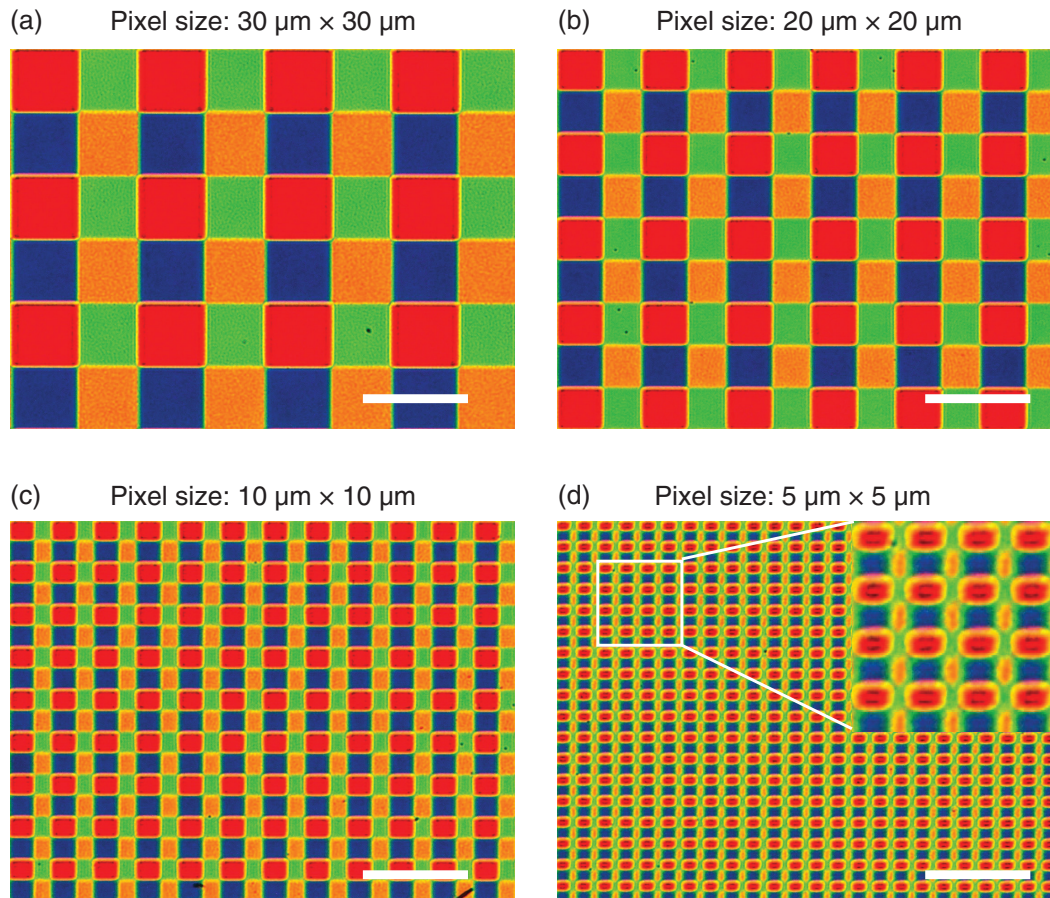
Fig. 5 The microscopy images of the color filter arrays made of pixelated F–P cavities. (a)–(d) The working wavelengths of the four kinds of color filters are 669 nm (red), 591 nm (yellow), 545 nm (green), and 468 nm (blue). The pixel sizes in (a)–(d) are 30 μm × 30 μm, 20 μm × 20 μm, 10 μm × 10 μm, and 5 μm × 5 μm, respectively. Scale bar: 50 μm.

10 μm [Fig. 5(c)], the color filter has a resolution of up to 1200 ppi, which is comparable to and even better than many commercial products. The resolution of the color filter can be further improved by precorrecting the proximity effect in the grayscale lithography.

3 Conclusions

We have demonstrated the fast manufacturing of large area color printing and color filter arrays by combing the concept of pixelated F–P cavities and the laser grayscale lithography technique. A centimeter scale F–P type color printing device with a spatial resolution of 5 μm × 5 μm and the 1/3-in. color filter arrays with resolutions higher than 1200 ppi were successfully fabricated. The transmission efficiency of the F–P cavities working in the visible regime is above 39%, which is comparable with many commercial color filters. With the proposed methods in this work, the pixel size can be smaller if the shorter wavelength laser and the objective lens with a larger numerical aperture can be used and the optical proximity effect during the exposure process is corrected. We expect that the proposed strategy in this work can be used for colorful painting, flat panel displays, hyperspectral imaging, and so on.

Data Availability

The data of this study are available from the corresponding author upon reasonable request.

References

1. A. Kristensen et al., "Plasmonic colour generation," *Nat. Rev. Mater.* **2**, 16088 (2016).
2. M. A. Kats et al., "Nanometre optical coatings based on strong interference effects in highly absorbing media," *Nat. Mater.* **12**, 20–24 (2013).
3. P. Hosseini, C. D. Wright, and H. Bhaskaran, "An optoelectronic framework enabled by low-dimensional phase-change films," *Nature* **511**, 206–211 (2014).
4. Z. -L. Deng et al., "Full-Color complex-amplitude vectorial holograms based on multi-freedom metasurfaces," *Adv. Funct. Mater.* **30**(21), 1910610 (2020).
5. T. Xu et al., "Plasmonic nanoresonators for high-resolution colour filtering and spectral imaging," *Nat. Commun.* **1**, 59 (2010).
6. Q. Chen and D. R. S. Cumming, "High transmission and low color cross-talk plasmonic color filters using triangular-lattice hole arrays in aluminum films," *Opt. Express* **18**(13), 14056–14062 (2010).
7. K. Kumar et al., "Printing colour at the optical diffraction limit," *Nat. Nanotechnol.* **7**, 557–561 (2012).
8. T. Ellenbogen, K. Seo, and K. B. Crozier, "Chromatic plasmonic polarizers for active visible color filtering and polarimetry," *Nano Lett.* **12**(2), 1026–1031 (2012).
9. S. J. Tan et al., "Plasmonic color palettes for photorealistic printing with aluminum nanostructures," *Nano Lett.* **14**(7), 4023–4029 (2014).
10. J. Xue et al., "Scalable, full-colour and controllable chromotropic plasmonic printing," *Nat. Commun.* **6**, 8906 (2015).
11. D. Franklin et al., "Actively addressed single pixel full-colour plasmonic display," *Nat. Commun.* **8**, 15209 (2017).
12. G. Li et al., "Near field imaging with resonant cavity lens," *Opt. Express* **18**(3), 2325–2331 (2010).
13. H. Shin et al., "Omnidirectional resonance in a metal–dielectric–metal geometry," *Appl. Phys. Lett.* **84**(22), 4421–4423 (2004).
14. J. D. Joannopoulos et al., *Photonic Crystals: Molding the Flow of Light*, 2nd ed., Princeton University Press, Princeton (2008).
15. Z. Dong et al., "Printing beyond sRGB color gamut by mimicking silicon nanostructures in free-space," *Nano Lett.* **17**(12), 7620–7628 (2017).
16. Y. Horie et al., "Visible wavelength color filters using dielectric subwavelength gratings for backside-illuminated CMOS image sensor technologies," *Nano Lett.* **17**(5), 3159–3164 (2017).
17. X. Zang et al., "Polarization encoded color image embedded in a dielectric metasurface," *Adv. Mater.* **30**(21), 1707499 (2018).
18. Y. Bao et al., "Full-colour nanoprint-hologram synchronous metasurface with arbitrary hue-saturation brightness control," *Light Sci. Appl.* **8**, 95 (2019).
19. H. Feng et al., "Spin-switched three-dimensional full-color scenes based on a dielectric meta-hologram," *ACS Photonics* **6**(11), 2910–2916 (2019).
20. W. Yang et al., "All-dielectric metasurface for high-performance structural color," *Nat. Commun.* **11**, 1864 (2020).
21. Y. Hu et al., "Trichromatic and tripolarization-channel holography with noninterleaved dielectric metasurface," *Nano Lett.* **20**(2), 994–1002 (2020).
22. X. Zhu et al., "Resonant laser printing of structural colors on high-index dielectric metasurfaces," *Sci. Adv.* **3**, e1602487 (2017).
23. Z. Yang et al., "Microscopic interference full-color printing using grayscale-patterned Fabry–Perot resonance cavities," *Adv. Opt. Mater.* **5**(10), 1700029 (2017).
24. Y. Chen et al., "Dynamic color displays using stepwise cavity resonators," *Nano Lett.* **17**(9), 5555–5560 (2017).
25. S. J. Kim et al., "Generation of highly integrated multiple vivid colours using a three-dimensional broadband perfect absorber," *Sci. Rep.* **9**, 14859 (2019).
26. S. D. Rezaei et al., "Direct color printing with an electron beam," *Nano Lett.* **20**(6), 4422–4429 (2020).
27. P. Mao et al., "Manipulating disordered plasmonic systems by external cavity with transition from broadband absorption to reconfigurable reflection," *Nat. Commun.* **11**, 1538 (2020).
28. C. Dai et al., "Stepwise dual-fabry–pérot nanocavity for grayscale imaging encryption/concealment with holographic multiplexing," *Adv. Opt. Mater.* **9**(21), 2100950 (2021).
29. Y. Wang et al., "Stepwise-nanocavity-assisted transmissive color filter array microprints," *Research* **2018**, 8109054 (2018).
30. Y. Hu et al., "3D-Integrated metasurfaces for full-colour holography," *Light Sci. Appl.* **8**, 86 (2019).
31. C. Williams et al., "Grayscale-to-color: scalable fabrication of custom multispectral filter arrays," *ACS Photonics* **6**(12), 3132–3141 (2019).
32. Thorlabs, Inc., "Compact scientific digital cameras user guide," pp. 24–25, 15 Jun 2022, https://www.thorlabschina.cn/drawings/9d740adb48335e3e-FC772B33-91B6-4CE5-4E3EBBE5D37D5C78/CS165MU-Manual.pdf
33. H. R. Miller, "Color filter array for CCD and CMOS image sensors using a chemically amplified thermally cured pre-dyed positive-tone photoresist for 365-nm lithography," *Proc. SPIE* **3678**, 1083–1090 (1999).
34. J. Guerrero et al., "Dyed red, green, and blue photoresist for manufacture of high-resolution color filter arrays for image sensors," *Proc. SPIE* **5017**, 298–306 (2003).
35. L. Jiang et al., "Microfabrication of a color filter array utilizing colored SU-8 photoresists," *Appl. Opt.* **59**(22), G137–G145 (2020).
36. A. D. Rakić et al., "Optical properties of metallic films for vertical-cavity optoelectronic devices," *Appl. Opt.* **37**(22), 5271–5283 (1998).
37. D. Malacara, *Color Vision and Colorimetry: Theory and Applications*, 2nd ed., SPIE Press, Bellingham (2011).

Yu Chen is a PhD student at Southern University of Science and Technology and Hong Kong Baptist University (joint PhD program), China. She received her bachelor's and master's degrees from Northeastern University, Shenyang, and Southern University of Science and Technology, Shenzhen, in 2019 and 2021, respectively. Her research interests include nano-optics, diffractive optical elements, and nano-fabrication.

Yang Li is a PhD student at Dalian University of Technology, Dalian, China. Since 2018, he has been studying as a visiting PhD student at Southern University of Science and Technology, Shenzhen, China. He received his bachelor's and master's degrees from Shandong University, Weihai, China, and DLUT in 2013 and 2017, respectively. His research interests include plasmonic metasurface and nonlinear optics.

Wenhao Tang is currently an engineer at Research Center for Humanoid Sensing, Zhejiang Lab, Hangzhou, China. He received his bachelor's degree from the School of Materials Science and Engineering, Shanghai Jiao Tong University, Shanghai, China, in 2020. He received his master's degree from the Department of Materials Science and Engineering, Southern University of Science and Technology, Shenzhen, China, in 2022. His research interests include color filter and bionic vision.

Guixin Li is a professor in nanophotonics in the Department of Materials Science and Engineering, Southern University of Science and Technology, China. He was awarded the 2019 Qiushi Outstanding Young Scholar of China. He has published around 100 peer-reviewed papers in high impact journals, such as *Nature Materials*, *Nature Nanotechnology*, *Nature Photonics*, *Nature Physics*, *Nature Reviews Materials*, and so on.

Biographies of the other authors are not available.